https://doi.org/10.5194/wcd-2020-39
Preprint. Discussion started: 19 August 2020

Weather and Climate Dynamics Discussions
Open Access
EGU

Oceanic origins for wintertime Euro-Atlantic blocking

Ayako Yamamoto[1,2], Masami Nonaka[1], Patrick Martineau[1,2], Akira Yamazaki[1], Young-Oh Kwon[3], Hisashi Nakamura[1,2], and Bunmei Taguchi[4]

[1]Japan Agency for Marine-Earth Science and Technology (JAMSTEC), Yokohama, Japan
[2]Research Center for Advanced Science and Technology, The University of Tokyo, Tokyo, Japan
[3]Woods Hole Oceanographic Institution, Woods Hole, MA, USA
[4]Faculty of Sustainable Design, University of Toyama, Toyama, Japan

Correspondence: Ayako Yamamoto (ayako.yamamoto@jamstec.go.jp)

Abstract. Although conventionally attributed to dry dynamics, increasing evidence points to a key role of moist dynamics in the formation and maintenance of blocking events. The source of moisture crucial for these processes, however, remains elusive. In this study, we identify the moisture sources responsible for latent heating associated with the wintertime Euro-Atlantic blocking events detected over 31 years (1979-2010). To this end, we track atmospheric particles backward in time from the blocking centres for a period of 10 days, using an offline Lagrangian dispersion model applied to an atmospheric reanalysis data.

The analysis reveals that 36 - 55% of particles gain a massive amount of heat and moisture from the ocean over the course of 10 days. Via large-scale ascent, these moist particles transport low potential vorticity (PV) air of low-altitude, low-latitude origins to the upper troposphere where the amplitude of blocking is the most prominent, consistent with the previous studies. PV of these moist particles remains significantly lower compared to their dry counterparts throughout the course of 10 days, preferentially constituting blocking cores.

Further analysis reveals that approximately two-thirds of the moist particles source their moisture locally from the Atlantic, while the remaining one-third from the Pacific. The Gulf Stream and Kuroshio and their extensions, as well as the eastern Pacific northeast of Hawaii, not only provide heat and moisture to the particles but also act as “springboards" for their large-scale, cross-isentropic ascent. While the particles of the Atlantic origin swiftly ascend just before their arrival at the blocking, those of the Pacific origin ascend additional few days earlier, after which they carry low PV in the same manner as dry particles. Thus, our study reveals that what may appear to be a blocking maintenance mechanism governed by dry dynamics alone can, in fact, be of moist origin.

https://doi.org/10.5194/wcd-2020-39
Preprint. Discussion started: 19 August 2020

Weather and Climate Dynamics Discussions
Open Access
EGU

1 Introduction

Atmospheric blocking is a large-scale, quasi-stationary anticyclonic circulation system, which acts to effectively “block" the prevailing westerlies (Rex, 1950) and divert synoptic disturbances (Booth et al., 2017). Blocking has garnered much attention due to its close association with the extreme weather events, such as cold spells in wintertime and heat waves and droughts in summertime, owing to its persistent nature. Despite these large socio-economic impacts, a comprehensive theory of the governing physical mechanisms behind the blocking life cycle remains elusive (Davini and D’Andrea, 2016; Woollings et al., 2018), and there remain biases in most climate models, leading to uncertainties in future projections of blocking activities (Woollings et al., 2018).

The dynamical processes behind blocking events have conventionally been attributed to dry processes. Previous studies demonstrate that the onset and maintenance of blocking often results from quasi-stationary Rossby wave propagation (Nakamura, 1994; Nakamura et al., 1997) and breaking (e.g. Pelly and Hoskins, 2003; Nakamura and Fukamachi, 2004; Masato et al., 2012), while the blocking longevity is maintained also by the contribution of feedback from the synoptic-scale migratory eddies (e.g. Shutts, 1983; Nakamura et al., 1997; Yamazaki and Itoh, 2013a).

A growing body of evidence from recent studies, however, points towards the importance of diabatic processes. In particular, a key role of latent heating associated with cloud formation in both the formation and maintenance stages of the blocking events has been highlighted. Latent heating augments vertical motion such that low potential vorticity (PV) air of low-altitude, low-latitude origin is efficiently transported to a high-altitude, high-latitude domain with high background PV, where a blocking forms (Wernli and Davies, 1997; Croci-Maspoli and Davies, 2008; Grams et al., 2011). This transport of low PV anomalies can also act to initiate an upper-level ridge and thereby modify a Rossby wave pattern (Grams et al., 2011; Methven, 2015), which may trigger a blocking formation. The most vigorous latent heating in the mid-latitude typically takes place in a warm conveyor belt (WCB), a rapidly ascending airstream associated with extratropical cyclones (Madonna et al., 2014). This cross-isentropic transport by the WCB can effectively inject low PV air into the upper troposphere, thereby intensifying the blocks (Pfahl et al., 2015; Steinfeld and Pfahl, 2019). This direct diabatic effect on blocking events has been shown to be of comparable importance to the dry processes in blocking dynamics (Pfahl et al., 2015), in particular for the wintertime Euro-Atlantic blocking systems (Steinfeld and Pfahl, 2019). In addition to this direct diabatic effect, Steinfeld and Pfahl (2019) further revealed an indirect diabatic effect, in which the vertical motion amplified by latent heating acts to enhance divergent outflow on the western flank of the blocking. This augmented divergent outflow in turn advects low PV anomalies on the western flank of blocking, thereby promoting the amplification and the westward expansion of blocking. Thus, these previous studies have elucidated the key role of latent heating in blocking systems. The source of the water vapour imperative to latent heating, however, is yet to be identified.

The largest source of atmospheric water vapour is irrefutably the ocean, and previous studies have uncovered its crucial role in blocking. For instance, Croci-Maspoli and Davies (2008) illustrated the high sensitivity of the formation of the European blocking to the imposed sea surface temperature (SST) and humidity over the North Atlantic basin in a high-resolution model, such that the higher SST and humidity content promote larger-scale block formation. In line with this result, Scaife et al.

https://doi.org/10.5194/wcd-2020-39
Preprint. Discussion started: 19 August 2020

(2011) found that a reduced mean Atlantic SST bias considerably improves blocking climatology over the Atlantic in a coupled climate model, although this improvement may be model dependent (Davini and D'Andrea, 2016). A recent study by Kwon et al. (2020) further corroborated the role of SST by showing that the multidecadal North Atlantic SST variability modulates the frequency of wintertime European blocking, whose covariability with the North Atlantic SST was first identified by Häkkinen et al. (2011). Kwon et al. (2020) suggested that this modulation of blocking is achieved through the mechanism discussed in Novak et al. (2015), in which poleward transient eddy heat flux in the lower troposphere is regulated by the underlying sharp SST gradients, resulting in the shift of the eddy-driven jet and a change in the dominant type of the Rossby wave breaking.

Other studies have attributed the oceanic influence on blocking specifically to the western boundary currents. Western boundary currents, such as the Gulf Stream in the North Atlantic and Kuroshio in the North Pacific in the Northern Hemisphere, are the swift ocean currents that transport a massive amount of heat poleward. Consequently, these are the regions where the exceptionally strong air-sea interactions take place by giving off large amount of heat and moisture to the overlying atmosphere (e.g. Kwon et al., 2010). By forcing an atmospheric general circulation model with realistic and smoothed Gulf Stream SST, O'Reilly et al. (2016) found that the sharp gradient of SST associated with the Gulf Stream acts to significantly amplify the wintertime Atlantic blocking, by reinforcing both the storm track and eddy-driven jet. Using an analogous experimental setup, Sheldon et al. (2017) showed that the Gulf Stream amplifies the deep cross-isentropic ascent, enabling a more efficient low PV transport from low-latitude, low-altitude regions. Furthermore, both Atlantic and Pacific blocks have been shown to sensitively respond to the interannual to decadal meridional variability of the Gulf Stream (Joyce et al., 2019) and the Kuroshio Extension (O'Reilly and Czaja, 2015), respectively. Thus, it is anticipated that the ocean and, in particular, the western boundary currents can play an important role in blocking events through moist processes.

The goal of the current study is to identify the oceanic sources of moisture fuelling wintertime Euro-Atlantic blocking events as a direct diabatic effect. To this end, we employ a Lagrangian method where we track atmospheric particles from the Euro-Atlantic blocking systems following three-dimensional wind fields backward in time. Unlike previous studies, we utilize an atmospheric Lagrangian dispersion model which allows us to investigate the processes taking place within the turbulent planetary boundary layer. In doing so, we aim to gain further insights into the moist processes affecting blocking events.

The rest of the paper is organized as follows. The dataset and methods used in this study are described in Section 2. In Section 3 we classify the particles released from blocking regions into the moist and the dry particles and examine their properties, while in Section 4 we further classify the moist particles based on their moisture sources and investigate their characteristics. A brief comparison of diabatic processes between Euro-Atlantic blocking and Pacific blocking is given in Section 5, followed by a discussion and conclusion drawn in Section 6.

2 Dataset and methods

2.1 Dataset

We use the Climate Forecast System Reanalysis (CFSR; Saha et al., 2010) datasets from the U.S. National Centers for Environmental Prediction (NCEP) for the period of 1979 to 2010 for our analyses. CFSR makes an ideal input for our Lagrangian

https://doi.org/10.5194/wcd-2020-39
Preprint. Discussion started: 19 August 2020

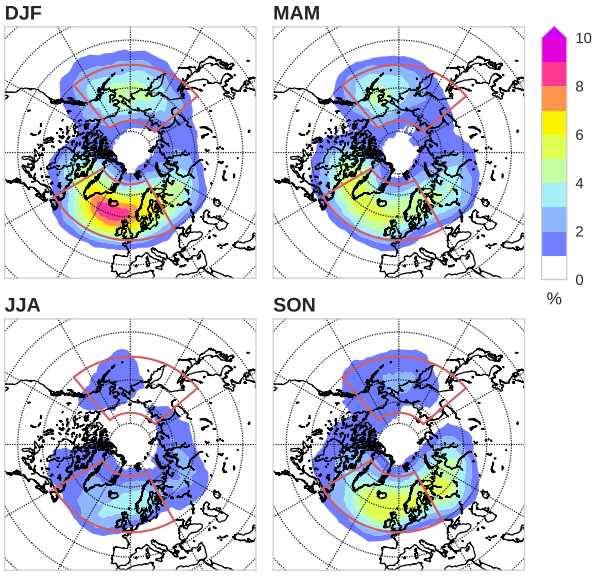

Figure 1. Seasonal climatology of the Northern Hemisphere blocking frequency over 1979 - 2010. Colour shading indicates the percentage of blocking days per season for each 2° × 2° grid cell. Red contours delimit the sector used to define the Euro-Atlantic blocks (60°W - 30°E, 50°N - 75°N) as well as the Pacific blocks (130°E - 140°W, 50°N - 75°N).

method, due to its high temporal and spatial resolutions of an hourly output with 0.5° horizontal resolutions and 37 vertical levels.

2.2 Blocking index

In the current study, we identify blocks using a hybrid index introduced by Dunn-Sigouin et al. (2013). This index combines two classical blocking definitions, whereby it searches for persistent, adjoining areas of positive 500-hPa geopotential height anomalies that are accompanied by a reversal of meridional geopotential height gradient (see Appendix A for more details). Thus, this index ensures the identified blocking to manifest the well-recognized properties of the anticyclonic circulation anomaly with the associated wind reversal, while suppressing the erroneous detection of quasi-stationary ridges and immature systems as blocking events (Dunn-Sigouin et al., 2013). Note that this detection method identifies blocking events as they reach maturity; thus, our analysis emphasizes processes associated with their mature stage rather than their development.

The seasonal climatological blocking frequencies thus detected are shown in Figure 1. Consistent with the previous studies, the maximum blocking frequencies are found during wintertime over the Atlantic and Pacific, while the minimum is found during summertime. As described in the introduction, we focus on the Euro-Atlantic blocks identified over [60°W - 30°E, 50°N - 75°N] in the December-January-February (DJF) season in the rest of our analyses, where the maximum blocking occurrence is found.

https://doi.org/10.5194/wcd-2020-39
Preprint. Discussion started: 19 August 2020

Weather and Climate Dynamics Discussions
Open Access
EGU

2.3 Trajectory computation

So-called atmospheric particles, representing infinitesimally small air parcels (Stohl et al., 2005), are tracked backward in time using an atmospheric dispersion model, FLEXPART version 9.0.3 (Stohl et al., 2005), from the Euro-Atlantic blocking area identified with the blocking definition introduced in the previous section.

FLEXPART computes the particle trajectories by adding parameterized sub-grid scale wind fluctuations to the resolved winds at every time step (see Appendix B for more details of how these sub-grid scale winds are computed in the model). This aspect of the dispersion model makes it markedly different from conventional kinematic trajectory models used by previous studies (e.g., Pfahl et al., 2015; Steinfeld and Pfahl, 2019), in which parcels are advected with resolved winds without taking into account the turbulent effects. As the purpose of the current study is to identify the role of the ocean in providing heat and moisture to the atmospheric particles which takes place within the turbulent planetary boundary layer (PBL), the inclusion of the turbulence effects makes FLEXPART an appropriate tool for the scope of the current study.

Using FLEXPART, we release 20 particles randomly placed in every 2.5 degree by 2.5 degree horizontal grid cell where and when Euro-Atlantic blocks have been identified. Assuming that blocking has an equivalent barotropic structure, the particles are released from the altitudes of between 7,000 and 8,000 m above the sea level (asl; corresponding to approximately 350 hPa on average), given that the amplitude of blocking anomalies maximizes in the upper troposphere (Dole and Gordon, 1983; Schwierz et al., 2004). As such, we have released a total of over five million particles from the interior of the DJF Euro-Atlantic blocking events for the whole 31 years. After the release, each of these particles is tracked backward in time for a duration of 10 days. Multiple atmospheric variables, including temperature, specific humidity, and air density, are interpolated at the particle's position at each time step, while additional meteorological quantities useful for the subsequent analyses, such as potential vorticity, PBL height, are computed in FLEXPART along each trajectory. Additionally, we have also released particles from lower altitudes of between 4,500 and 5,500 m asl and between 3,000 and 4,000 m asl, approximately corresponding to 500 hPa and 700 hPa, respectively.

Furthermore, following Yamamoto et al. (2015) and Yamamoto and Palter (2016), whenever the particles reside within the atmospheric PBL over the ocean, we interpolate surface heat flux (SHF) and latent heat flux (LHF) at the particle's 6-hourly location and time. These turbulent heat fluxes are useful in evaluating where the particles that eventually reach the Euro-Atlantic blocks are likely to be supplied with heat and moisture from the ocean.

3 Distinct characteristics of the moist and the dry particles

In order to elucidate the role of the ocean in providing moisture to the atmospheric particles en route to the Euro-Atlantic blocks, we first partition the individual particles into the moist and the dry particles. Here, the moist particles are defined as those that are subject to evaporation from the ocean, evaluated with positive value of LHF, for at least one time step over the course of 10 days. Otherwise, the particles are regarded as dry particles. As our goal lies in identifying the oceanic sources of moisture for the blocking particles, we opt for this definition based on the moisture gain from the ocean over that used in Pfahl

https://doi.org/10.5194/wcd-2020-39
Preprint. Discussion started: 19 August 2020

et al. (2015) and Steinfeld and Pfahl (2019), who defined the diabatic particles as those that are heated by more than 2 K within three days prior to their arrival in the blocking regions.

With our definition, we have identified 36.4% of the total particles as moist particles and 63.6% to be dry particles. This fraction of the moist particles in our study falls within the range of diabatic particles of 30 - 45% reported by Pfahl et al. (2015), while it is underestimated compared to their fraction of 60 - 70% when the 7-day period is considered. We speculate that this difference might arise from the difference in the definition of the moist particles and/or the fact that Pfahl et al. (2015) primarily used the anomaly-based blocking definition by Schwierz et al. (2004), which can also detect immature/onset stages of blocking unlike the current study, when the direct diabatic effect tends to maximize (Pfahl et al., 2015; Steinfeld and Pfahl, 2019). In contrast, the fraction reported by the previous studies during the maintenance stage seems fairly consistent with the current study (see Figure 6 of Steinfeld and Pfahl, 2019). When we release the particles from the lower altitudes, the fraction of moist particles increases to 49.7% and 55.0% for the 5,000 m asl and 3,500 m asl release, respectively.

3.1 Spatial distribution of the moist and the dry particles

The spatial distributions of the moist and the dry particles 2, 5, and 9 days prior to their arrival at the blocking locations are shown in Figure 2, where the particle release locations (i.e. where blocking occurs, corresponding to day 0) are indicated by red contours. As shown in Figure 2, the particles in both categories are mostly advected eastward under the prevailing westerlies. Compared to their moist counterpart, dry particles tend to travel slightly faster. This faster advection rate for the dry particles reflects their tendency to be situated at higher altitudes (see Section 3.3), where the background westerlies tend to be swifter.

Upon further inspection of Figure 2, one notices that moist particles 9 days prior (upper-right panel) tend to be situated within two distant regions separated by the Rockies, seemingly corresponding to the two major storm tracks in the wintertime Northern Hemisphere. Meanwhile, the maximum particle density 2 days prior is found over the midlatitude North Atlantic just south-west of the blocking region, which is an important ascent region for some of these moist particles, as will be shown later. In contrast, the corresponding locations of the dry particles appear to be less concentrated. As such, it is speculated that these two categories of particles tend to undergo different dynamical processes.

3.2 Spatial distribution of mean properties along the moist particles within and above the marine PBL

We further partition the moist particles into the time when they are located within the atmospheric PBL over the ocean (Figure 3) and the rest of the time (Figure 4), in order to unambiguously identify the role of the ocean in fuelling the moist particles. As such, Figure 3 illustrates where the particles are located and how the mean properties along them are distributed when the moist particles can exchange heat and moisture with the underlying ocean, while Figure 4 shows when those particles are not in direct contact with the ocean. Note that the latter also includes the time when the particles are located within the PBL over land.

Figure 3a reveals that the moist particles preferentially stay within the PBL over the Gulf Stream and/or the Kuroshio as well as their extensions, where they tend to be both heated (Figure 3b) and moistened (Figure 3c) through the enhanced upward turbulent heat fluxes (Figure 3b,c; yellow contours). These results suggest a central role of the western boundary currents

https://doi.org/10.5194/wcd-2020-39
Preprint. Discussion started: 19 August 2020

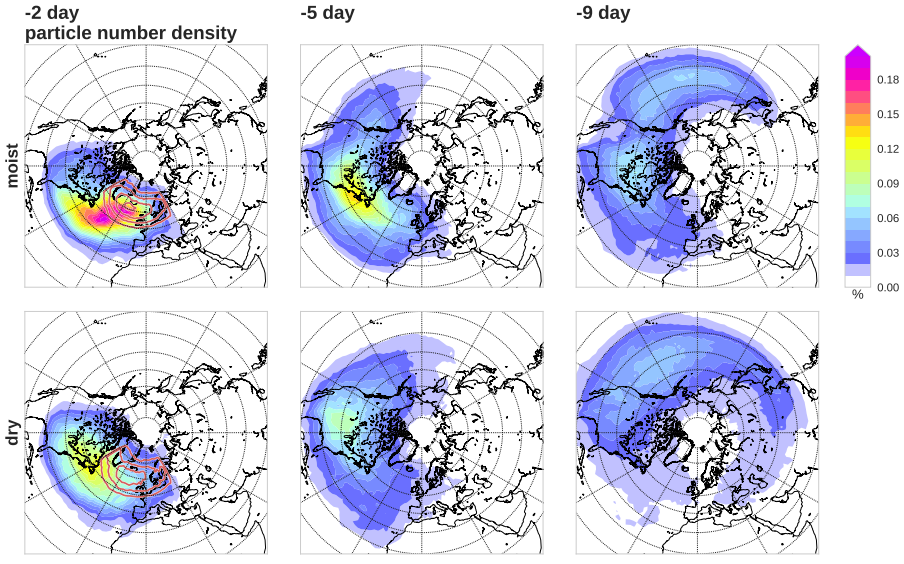

Figure 2. Number density for each 2° × 2° grid cell for the moist particles (top) and dry particles (bottom) 2 days (left column), 5 days (middle column), and 9 days (right column) prior to their arrival at the wintertime Euro-Atlantic blocking highs. Red contours denote the location of the particle release location (i.e. where the blocks form) with the interval of 0.05% starting from 0.1%. In each panel the sum of all grid cells is 100%.

as the primary heat and moisture sources for the moist particles that are going to be advected into the Euro-Atlantic blocks. One noticeable exception to this overall tendency is found off the west coast of North America, where the particles undergo topographical lifting (Figure 3d) followed by dehydrating (Figure 3c) and warming (Figure 3b) due to latent heating. As will be shown later in Section 4.3, this region turns out to be a common location for the organized large-scale ascent of the particles that gain moisture from the Pacific.

In stark contrast, the dominant tendency for the moist particles when situated above the PBL (Figure 4) is such that an increase (decrease) in potential temperature is concurrent with a decrease (increase) in specific humidity, which is accompanied by their ascent (descent) (Figure 4d). This result means that latent heating and evaporative cooling are the dominant processes that control the property changes of the particles travelling above the PBL. The preferred locations for the particle ascent are found just upstream of the blocking over the North Atlantic 2 days prior to their arrival at the blocking region, as well as off the west coast of the North American continent, found 5 and 9 days prior to the arrival at the blocking.

Meanwhile, the dry particles undergo barely any property change, except for a general cooling trend associated with radiative cooling (not shown).

https://doi.org/10.5194/wcd-2020-39
Preprint. Discussion started: 19 August 2020

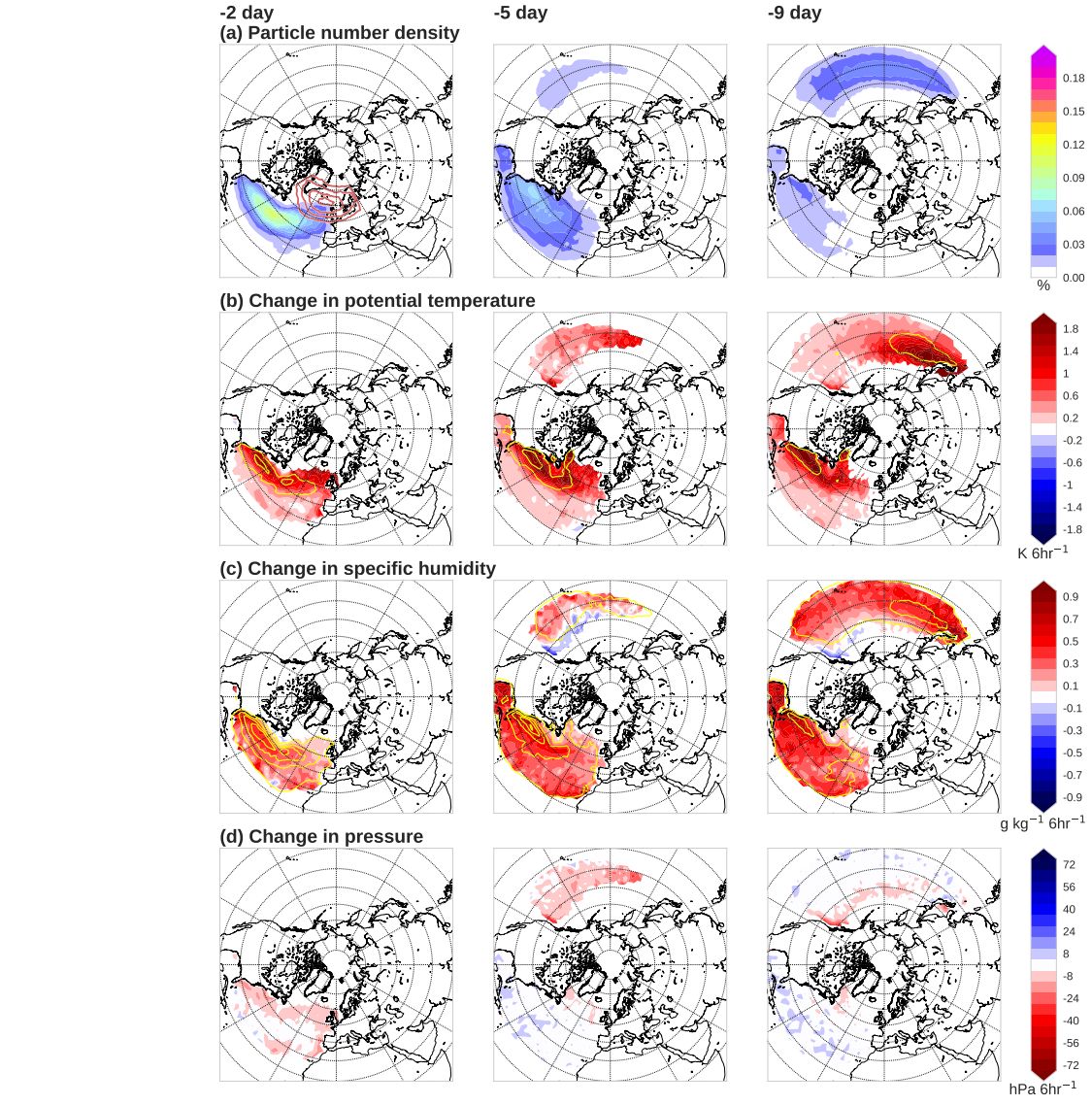

Figure 3. Properties along the moist particles when they are located within the marine PBL 2 days (left column), 5 days (middle column), and 9 days (right column) prior to their arrival at the Euro-Atlantic blocks. (a) Number density of the particles for each $2^\circ \times 2^\circ$ grid cell, with their release locations being indicated by the red contours with the interval of 0.05% starting from 0.1%. (b) Mean change in potential temperature (colour shading), with SHF for the particles accumulated for each $2^\circ \times 2^\circ$ grid cell and normalized by the number of the moist particles at each time lag (yellow contours indicating 0.01, 0.05 W m^{-2}) superimposed. (c) Mean change in specific humidity (colour shading) with accumulated LHF overlaid (yellow contours for 0.01, 0.05, 0.1 W m^{-2} with the interval of 0.05 W m^{-2} afterwards). (d) Mean change in atmospheric pressure. For (b) - (d), only those grid cells that contain over 0.005% of the total particle's 6 hourly density are plotted).

https://doi.org/10.5194/wcd-2020-39
Preprint. Discussion started: 19 August 2020

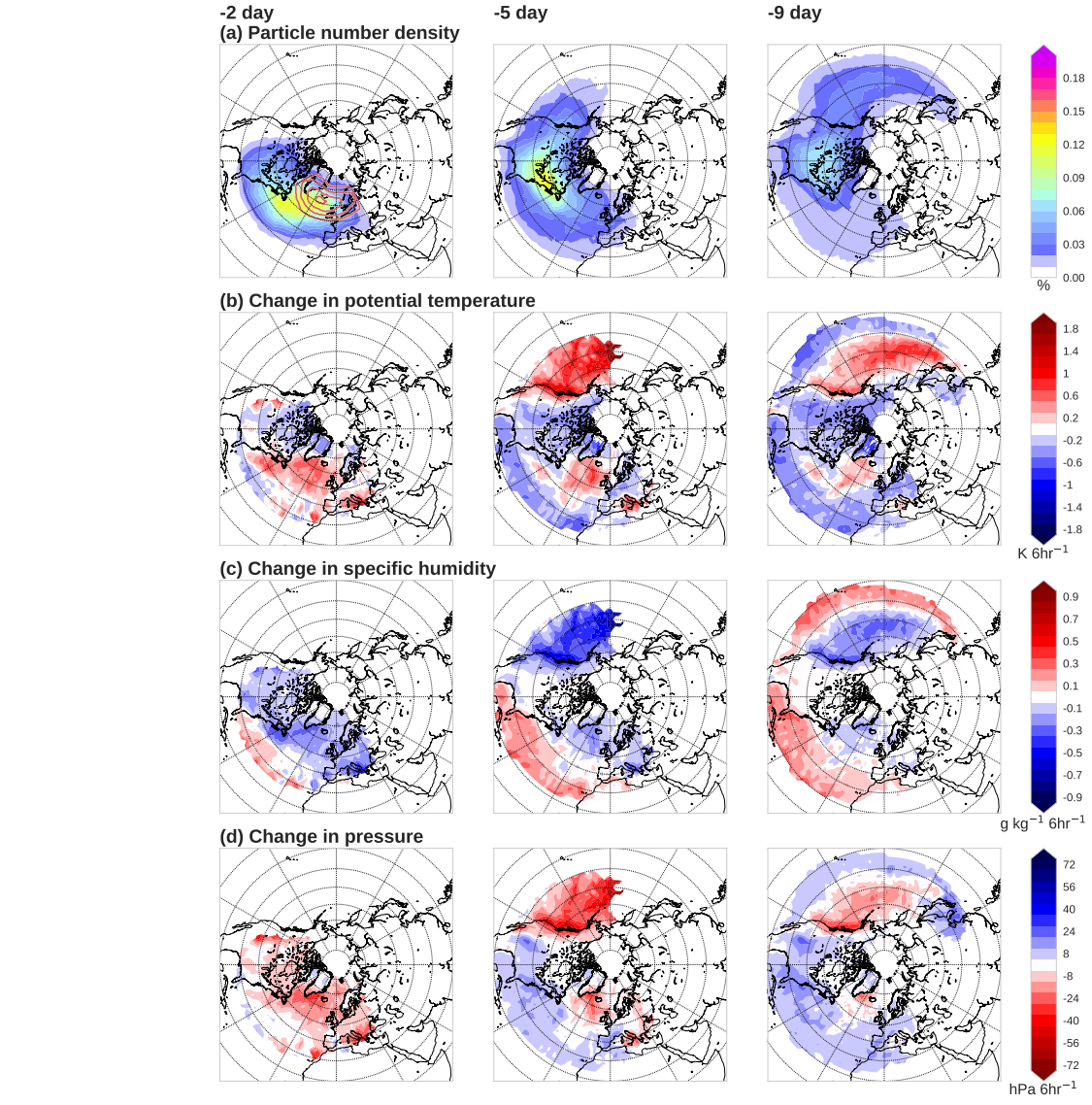

Figure 4. Same as Figure 3, but for the moist particles when located above the marine PBL, including those moist particles that are located within the PBL over land. By definition they are not under the influence of the turbulent heat fluxes from the ocean.

3.3 Time evolution of variables along the trajectories of the moist and the dry particles

In order to further understand different properties associated with the dry and the moist particles, we compare the mean temporal evolution of several variables along their trajectories.

Figure 5 reveals that dry particles (cyan lines) tend to originate from the midlatitudes and advance gradually northward, while travelling pseudo-isobarically in the upper troposphere. These particles undergo a cooling of approximately 0.7 K day^{-1},

https://doi.org/10.5194/wcd-2020-39
Preprint. Discussion started: 19 August 2020

Weather and Climate Dynamics Discussions
Open Access
EGU

consistent with the radiative cooling reported by Steinfeld and Pfahl (2019). Specific humidity of the dry particles is fairly low over the course of 10 days en route to the blocking regions, as these particles do not pick up any moisture from the ocean by definition. Despite its large standard deviation, PV of the dry particles is maintained around approximately 2 PVU (potential vorticity unit; 1 PVU $\equiv 1.0 \times 10^{-6}$ m^2 s^{-1} K kg^{-1}), a typical PV value at the dynamical tropopause.

Moist particles (red lines in Figure 5) display a fairly distinct picture from its dry counterparts: While also originating from the mid-latitudes and travelling northward, the moist particles tend to arise from the lower troposphere and then undergo a substantial uplift over the course of 10 days. This uplift and the northward motions are particularly enhanced about 3 days prior to their arrival at the blocking system, coinciding with notable dehydration and warming due to intense latent heating during this period. The mean PV of the moist particles tends to retain fairly low values throughout without undergoing any substantial changes, reflecting their origins at the lower altitudes and latitudes. Until about 3 days before their arrival at the blocks, the moist particles tend to be steadily supplied with SHF and LHF, before undergoing strong uplift.

Despite the aforementioned significant differences in their origins and their evolution between the dry and the moist particles, these differences almost diminish as time nears the particle release time from the blocks (i.e. particle age = day 0). One notable exception is PV, which on average undergoes little change during the course of 10 days, retaining its initial values along the trajectories of both dry and moist particles even at day 0. This result is consistent with the previous study by Methven (2015), who showed that the average PV of an upper-tropospheric outflow of a strongly ascending air stream is approximately equal to that of the lower-tropospheric inflow on average, as PV increases below the heating maximum but decreases above it. Figure 5 indicates that the mean PV values are significantly higher for the dry particles than for the moist particles at the 99% confidence level even at day 0. Given that blocks are high pressure systems associated with low PV values, feeding of lower PV air is expected to be crucial for their maintenance (Yamazaki and Itoh, 2013b). Our result thus suggests that these moist particles play an important role in transporting significantly lower PV into the block system, further corroborating the findings of the previous studies (Pfahl et al., 2015; Steinfeld and Pfahl, 2019).

This significant difference between the dry and moist particles in their mean PV values seen at day 0 in Figure 5 further suggests that there could be a difference in their spatial distribution at the time of their release from the blocks. Figure 6 illustrates the spatial distributions of the dry and moist particles separately, as well as their difference. Each row denotes different release altitudes: 7,500-m asl (∼350 hPa), 5,000-m asl (∼500 hPa), and 3,500-m asl (∼700 hPa). The figure reveals that regardless of the release altitudes, the density of the moist particle (middle panels) at the centre of the blocks tends to be higher than that of the dry particles (left panels). The difference plots (right panels) highlight that this difference is more apparent for the particles released from the lower altitudes (5,000 m asl and 3,500 m asl). The moist particles released from 7,500 m asl tend to be situated slightly to the east of the dry particles, indicating the possibility of vertically-slanted injection of moist particles, which may be a reflection of the slantwise nature of the WCB (Oertel et al., 2020). Overall, our results suggest that the moist particles act to transport the low PV across isentropic surfaces to the upper levels, such that a blocking core is preferentially constituted of moist particles with lower PV.

https://doi.org/10.5194/wcd-2020-39
Preprint. Discussion started: 19 August 2020

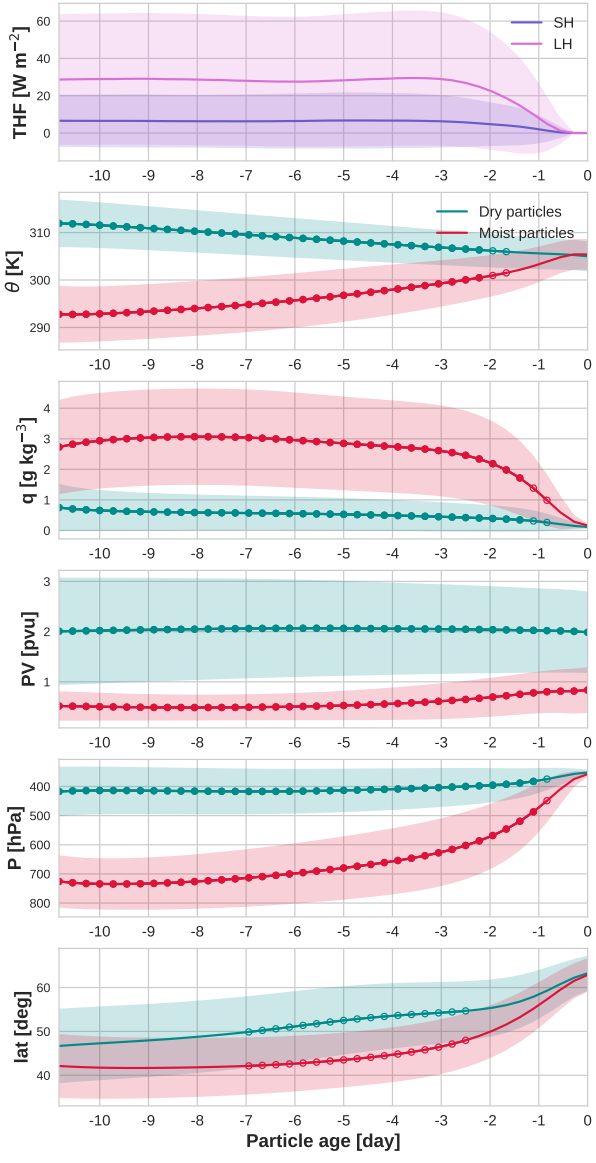

Figure 5. Time evolution of the properties of the dry and the moist particles along their respective trajectories. (Top) Mean sensible (blue) and latent heat fluxes (magenta) supplied for the moist particles from the ocean when the particles reside within the marine PBL. (Second to last rows) mean potential temperature (second row), mean specific humidity (third row), mean potential vorticity (fourth row), mean pressure (fifth row), and mean latitude (last row) of the dry (cyan lines) and moist particles (red lines) along their respective trajectories. The envelopes around each line indicate ± 0.5 standard deviation. The particle age on the x-axis denotes the days before the particles arrive at the blocking system (i.e., day 0 means the arrival time at the blocks). The closed (open) circles indicate where a given property distribution between the moist and dry particles is significantly different at the 99% (95%) confidence level.

https://doi.org/10.5194/wcd-2020-39
Preprint. Discussion started: 19 August 2020

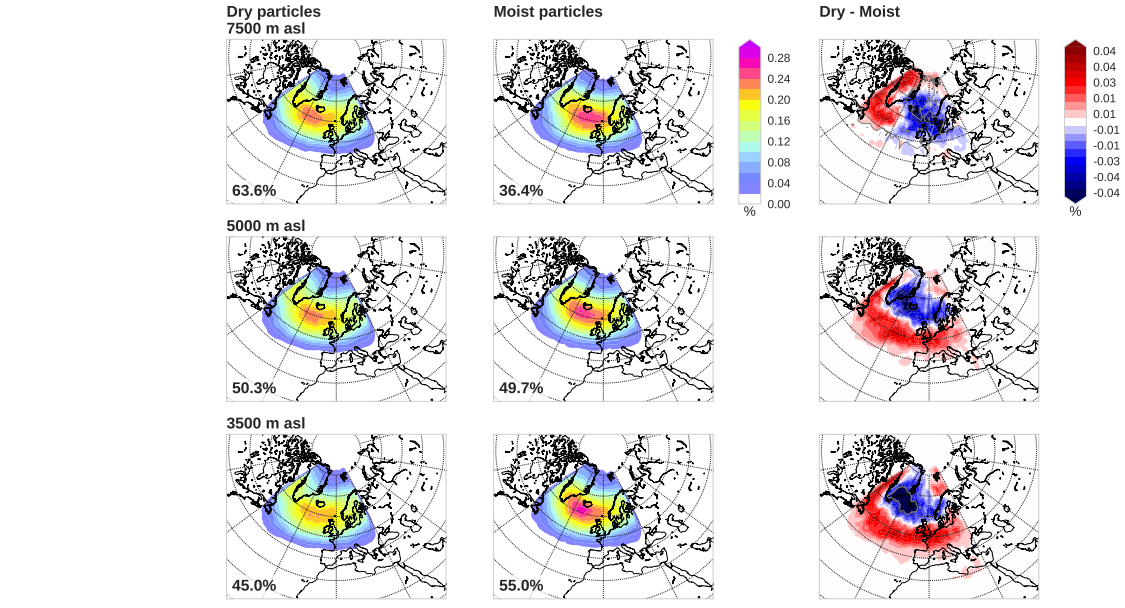

Figure 6. The number density of the dry (left column) and the moist particles (middle column) and their normalized difference (right column) for each $2^\circ \times 2^\circ$ grid cell at the time of their release from the block regions, separately for the release altitudes of 7,500 m asl (top), 5,000 m asl (middle row), and 3,500 m asl (last row). The numbers indicated on the bottom left corner for the left and middle columns denote the percentages of the dry and the moist particles released from each altitude, respectively. The regions encircled by the grey contours denote the regions of statistical difference significant at the 95% confidence level.

4 Moisture sources for the moist particles

In the previous section we found that heat and moisture for the moist particles are not only locally sourced from the Atlantic, but the North Pacific also likely acts to supply necessary heat and moisture to some particles en route to the Euro-Atlantic blocking (Figure 3). In this section, we further separate the moist particles depending on their moisture sources, in order to uncover the characteristics associated with their different pathways and their roles in blocking maintenance.

4.1 Partitioning of the moist particles according to their moisture sources

We partition the moist particles into the two different moisture origins based on the ocean basin mask dataset with 1° horizontal resolution provided by the U.S. National Oceanic and Atmospheric Administration (NOAA; https://iridl.ldeo.columbia.edu/SOURCES/.NOAA/.NODC/.WOA05/.Masks/.basin/index.html?Set-Language=en.). Those particles that are subject to LHF from the ocean over the Atlantic south of 65°N and the Mediterranean Sea are termed “Atlantic pathways", while those over the Pacific south of 65°N as well as the Sea of Japan are termed “Pacific pathways". As such, we have found that approximately two-thirds of the moist particles (i.e. 22.8% out of 36.4% of the total moist particles) source their moisture from the Atlantic basin, while the vast majority of the remaining one-third from the Pacific (i.e. 12.1% out of 36.4% of the total moist particles),

https://doi.org/10.5194/wcd-2020-39
Preprint. Discussion started: 19 August 2020

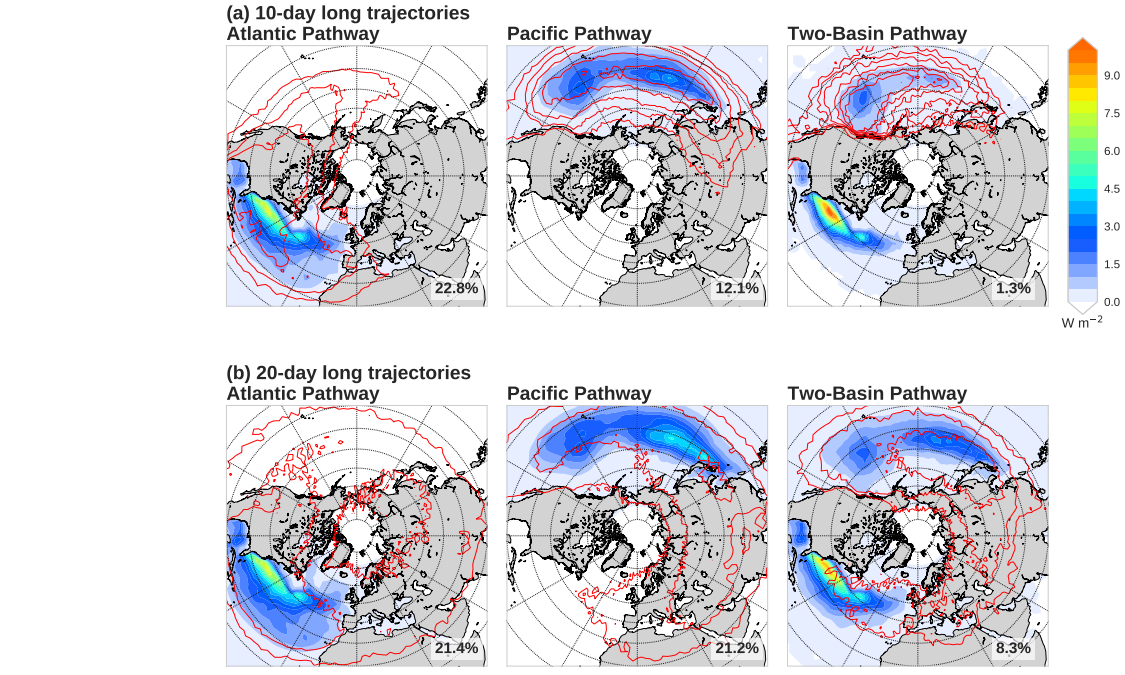

Figure 7. Latent heat flux accumulated for each 2° × 2° grid cell and normalized by the particle number for each moisture source category (colour shading), for the Atlantic pathways (left column), Pacific pathways (middle column), and two-basin pathways (right column), for (a) 10-day and (b) 20-day periods for backward particle tracking. The origin locations for each 2° × 2° grid cell is denoted by the red contours for 0.01, 0.025, 0.05, 0,1, 0.15, and 0.2% in each panel. The percentage indicated on the bottom right corner of each panel denotes the percentage of the particles that belong to each moisture source category, out of the total number of particles (i.e. dry and moist particles altogether).

when particles are tracked backward in time for the period of 10 days (Figure 7a). Intriguingly, a minute fraction of the particles (1.3% of the total moist particles) receive heat and moisture from both the Pacific and Atlantic basins (denoted "two-basin pathways"). Note that we do not consider the moist particles fuelled over the Indian Ocean in the rest of the analyses, which account for only 0.9% of the total moist particles. These particles do not additionally source moisture from the other basins (not shown).

When we extend the duration of the particle tracking from 10 days to 20 days (Figure 7b), however, the fraction of the moist particles increases by 40%, especially escalating the fraction of the Pacific pathways and two-basin pathways, while the 20-day tracking accounts for almost the same fraction as the Atlantic origin. The twofold increase of the Pacific pathway particles indicates that the 10-day period is not long enough for some particles to be traced back to their moisture source in the Pacific. The over sixfold increase of the two-basin pathways is explained primarily by the detection of additional particles of the Atlantic origin that previously stayed in the PBL over the Pacific between 10 and 20 days prior to blocking events, and to a lesser extent by some particles of the Pacific origin that are tracked back further to the Atlantic, across Eurasia. The fraction

https://doi.org/10.5194/wcd-2020-39
Preprint. Discussion started: 19 August 2020

of particles sourcing the moisture from the Indian Ocean remains lower than 1% even with the 20-day tracking, indicating that Indian Ocean does not act to provide much moisture for the wintertime Euro-Atlantic blocking events.

The Atlantic pathways tend to originate locally 10 days prior to the arrival at the block locations (the particle distribution at -10 days indicated by the red contours in Figure 7a), with their maximum concentration found over the lee side of the Rockies over the North American continent. These particles then pick up a substantial amount of moisture from the Gulf Stream and its extension. A similar picture holds when they are tracked for 20 days (Figure 7b), although more particles tend to stem from the east of the block locations over Eurasia.

The Pacific pathways identified through the 20-day tracking tend to originate from farther upstream, primarily receiving turbulent heat fluxes from the Kuroshio and its extension, with a clearer maximum concentrated along the Kuroshio Extension. Still, the accumulated LHF maximum along the Kuroshio Extension is only about half of that along the Gulf Stream, despite no notable difference in the climatological turbulent heat fluxes between them. It remains to be investigated whether this suppressed LHF would be enhanced with particle tracking beyond 20 days.

The origin locations of the two-basin pathways appear to be a mixture between the Atlantic and Pacific pathways, though largely stemming from the western Pacific. These particles tend to pick up ample moisture from the two western boundary currents and their extensions. Again, the role of the Kuroshio becomes more apparent when particles are tracked back for 20 days.

In addition, there exists another local maximum of the accumulated LHF around [30°N, 145°W] north-east of the Hawaiian Islands for both the Pacific and two-basin pathways (Figure 7 the middle and the right panels). Unlike the western boundary currents and their extensions, this particular region is not climatologically characterized by large upward LHF. The accumulated total LHF is affected by the following two factors: particles' 6-hourly concentrations and the actual LHF supplied to the particles. Further analysis indicates that these two factors both contribute, suggesting that the particles are preferentially situated over this location and that they are subject to a larger amount of LHF than its climatology (not shown). As discussed later in Section 4.3, this region coincides with starting locations of the large-scale ascent for those particles supplied with moisture from the Pacific, thus acting as a "springboard".

4.2 Time evolution of variables along the trajectories of particles of the different moisture sources

In order to assess whether physical processes involved depend on the particles' moisture sources, we repeat the same analysis on the temporal evolution of variables along the particle trajectories, but this time after separated into different moisture sources (Figure 8). Additionally, a three-dimensional view of the mean positions of these different pathways along with their mean PV value are shown in Figure 9 in order to illustrate their typical trajectories relative to their geographical locations.

Figure 8 reveals that the Atlantic pathways tend to originate from northern locations in the mid-troposphere on average (red lines). These particles gradually descend while travelling southward and gaining moisture until the last 3 - 4 days, before being lifted up swiftly and undergoing latent heating over the Atlantic basin (Figure 9).

In contrast, the Pacific pathways (orange lines in Figure 8) stem from the lower latitudes and altitudes. On the following days (day 9 - day 4) these particles keep ascending and experiencing latent heating, especially off the west coast of North America

https://doi.org/10.5194/wcd-2020-39
Preprint. Discussion started: 19 August 2020

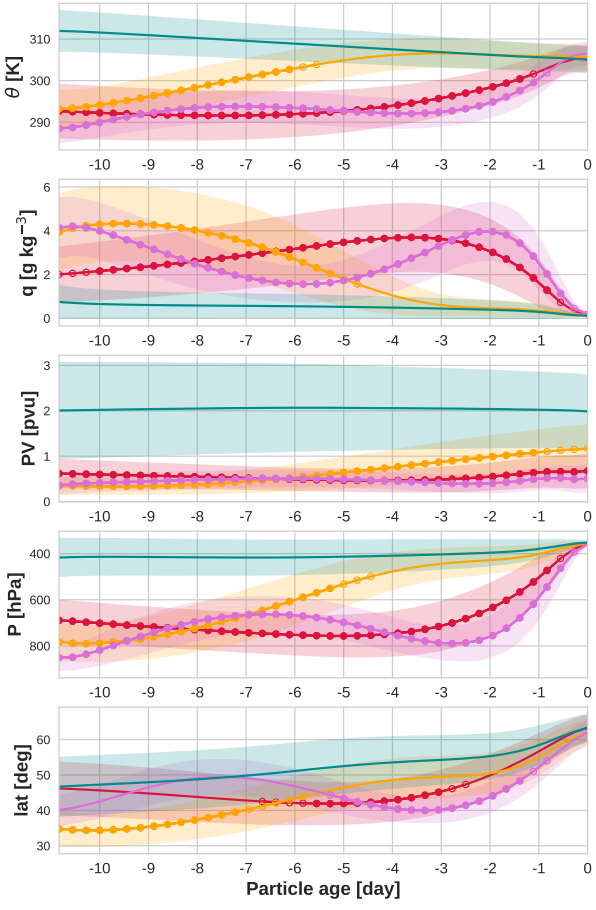

Figure 8. Same as Figure 5, but for the moist particles categorized according to their moisture sources: the Atlantic pathways (red), Pacific pathways (orange), and two-basin pathways (magenta). Cyan denotes the properties for the dry particles.

(Figure 9), which tends to occur earlier than the Atlantic pathways by approximately 4 - 5 days. After nearly all the moisture is lost by day -4, most of the properties of these particles become almost indiscernible from those of the dry particles (denoted by cyan lines), travelling along similar pressure and isentropic surfaces as well as at similar latitudes. In addition, they undergo radiative cooling at the same rate as the dry particles from then on. The Pacific pathway particles are thus transported in the same manner as the dry particles once lifted up into the mid-troposphere.

The two-basin pathways evolve in a similar manner to the Pacific pathways at the beginning (magenta lines in Figure 8), as the particles originate from relatively low latitudes and altitudes with relatively high moisture content and then undergo ascent over the Pacific, especially off the west coast of North America. The ascent is, however, only by about 150 hPa till day -7, leading to slight latent heating. As will be shown in Section 4.4, this lesser extent of uplift off the west coast of North America stems from the lower humidity content of those particles compared to the Pacific counterpart at the time of the ascent. These

https://doi.org/10.5194/wcd-2020-39
Preprint. Discussion started: 19 August 2020

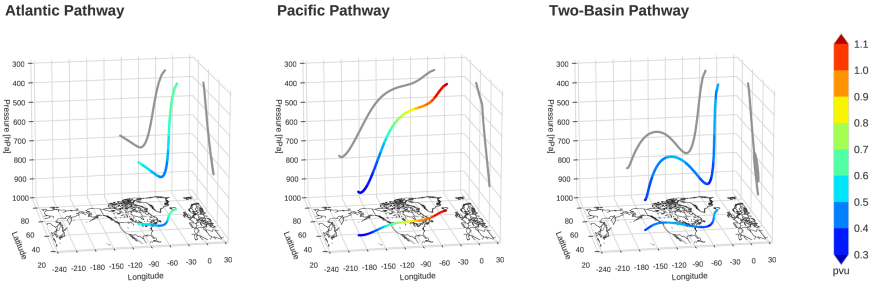

Figure 9. Three-dimensional trajectory locations averaged for the Atlantic pathways (left), Pacific pathways (middle), and two-basin pathways (right). The lines on the surfaces of constant pressure, latitude, and longitude are the projections of the three-dimensional mean trajectory locations on each surface. The colours along the trajectories denote the mean PV values.

particles then start descending on the lee side of the Rockies (Figure 9) and receive heat and moisture from the Atlantic, before ascending very rapidly into the blocking system in the last 2 days (Figure 8).

The PV values of the moist particles, regardless of their moisture sources, are significantly lower than those of the dry particles. In particular, although the Pacific pathways undergo a slight increase in PV after day -5, as they appear to be advected indistinguishably from the dry particles as noted earlier, their PV values are still significantly lower than those of the dry particles. When compared to the winter-mean background PV, the PV values of these particles in the last 4 days just before arriving at the blocking system indeed tend to be significantly lower, indicating that they are associated with anticyclonic eddies (Figure 10). This result further corroborates the previous findings that once lifted up into the upper troposphere these particles constitute low PV anomalies in contrast to the background upper tropospheric PV at the same location (Pfahl et al., 2015; Steinfeld and Pfahl, 2019). In light of the blocking mechanism, therefore, these moist particles can be considered as those associated with anticyclonic eddies (low PV) that are selectively absorbed into the blocking system (Yamazaki and Itoh, 2013a), acting to prolong the blocking lifetime. While Yamazaki and Itoh (2013a) identified the physical process in the upper troposphere through an isentropic trajectory analysis by implicitly assuming dry processes (Pfahl et al., 2015), our result points towards a reconciled view such that at least a part of this low PV air can, in fact, be traced back to moist processes farther upstream.

We have repeated the same analysis using particles tracked backward in time for 20 days. Extending the tracking time, however, does not change the qualitative picture shown in Figure 8, except that all categories of particles originate from the mid-latitudes. Despite that some particles are classified in different pathways under the extended tracking, the evolution of the properties during the last 10 days is indistinguishable from those obtained from the 10-day tracking (not shown), indicating the significance of the processes that take place in the final 10 days for the downstream blocking.

https://doi.org/10.5194/wcd-2020-39
Preprint. Discussion started: 19 August 2020

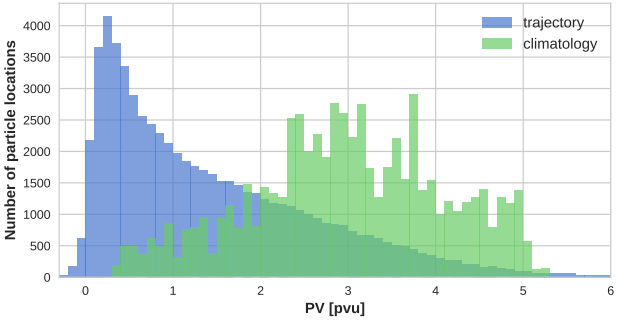

Figure 10. Probability density distributions of PV values for the Pacific pathways (blue) and for the climatological values interpolated at their two-dimensional locations (green). The former is based on 10.1% of the Pacific pathways that reached above 400 hPa and whose potential temperature remains between 300 K and 310 K in the last 4 days before arriving at the Euro-Atlantic blocks, while the latter on the CFSR climatological PV values at 305 K level computed as the DJF-mean for each winter. The two distributions are significantly different at the 95% confidence level.

4.3 Large-scale ascent associated with moist particles with different moisture sources

Given the importance of large-scale cross-isentropic ascent, here we investigate the extent of uplift as well as the associated properties for the moist particles with different moisture sources. Here, we quantify large-scale ascent in accordance with the definition of WCB. Following Steinfeld and Pfahl (2019), we define those particles that undergo a prominent rapid ascent for at least 600 hPa within 48 hours as the particles along the WCB. For simplicity, unlike Madonna et al. (2014), the particles are not required to be in the vicinity of cyclones to be identified as the WCB particles in our definition. Our WCB particles may thus include those particles that are not strictly classified as the conventional WCB. A detailed analysis of individual events, nonetheless, revealed that these events are almost always accompanied by cyclonic systems at the time of their ascent (not shown). Consistent with Madonna et al. (2014), the average increase in potential temperature associated with the WCB particles is found to be about 20 K, while the average decrease in specific humidity about 7 g kg^{-1}.

Figure 11 indicates that approximately 30% of the moist particles (i.e. about 10% of the total number of particles) is identified as the WCB particles at some point along their 10-day trajectories, regardless of their moisture sources. This number ($\sim$10%) is fairly similar to 9.7% reported by Steinfeld and Pfahl (2019), who considered a 7-day period. Meanwhile, this fraction is much larger than the finding by Madonna et al. (2014), who reported only 0.36% of the 2-day trajectories released for the period from 1979 to 2010 from the entire lower troposphere to be identified as the WCB trajectories. This difference in the fraction of the WCB trajectories from the climatology may thus indicate that the WCB trajectories are preferentially channeled towards the blocking systems. The fraction of the moist particles identified as WCBs exceeds above 60% (90%) of the total moist particles when the WCB definition is loosened to an ascent over 500 hPa (400 hPa) within 48 hours (Table 1).

Figure 11 illustrates that the ascent preferentially takes place around the western boundary currents and their extensions, as well as the eastern Pacific to the northeast of the Hawaiian Islands, just as was the case for the locations of the maximum

https://doi.org/10.5194/wcd-2020-39
Preprint. Discussion started: 19 August 2020

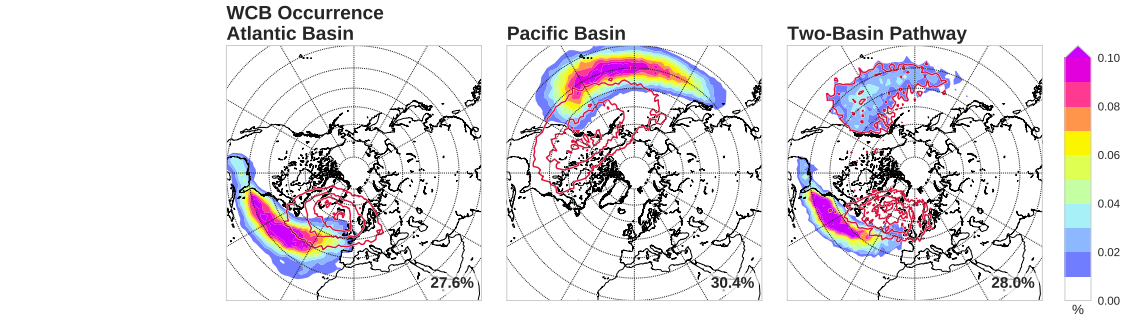

Figure 11. Number density of the WCB particles at the starting time of the ascent (colour shading) and its ending time of their ascent (red contours) for each 2° × 2° grid cell for the Atlantic pathways (left), the Pacific pathways (middle), and the two-basin pathways (right). The number at the bottom right of each panel indicates the fraction (%) of the particles of each category identified as WCB particles.

Table 1. The fractions of individual moist particle pathways which fulfill different ascent criteria.

Ascent Criterion	Atlantic Pathways	Pacific Pathways	Two-basin Pathways
600 hPa/48 hr	27.6%	30.4%	28.0%
500 hPa/48 hr	68.1%	63.8%	69.7%
400 hPa/48 hr	90.2%	86.8%	91.8%

accumulated LHF (Figure 7). These locations, including the region to the northeast of Hawaiian Islands agree with the reported climatological locations of the wintertime WCB occurrence (Madonna et al., 2014, their Figure 4d). This close collocation between the particles' acquisition of turbulent heat fluxes and their ascent is in line with the results shown by Boutle et al. (2010) in their idealized extratropical cyclone simulation. They showed that the augmented continuous evaporation is found in the vicinity of the WCB as a consequence of the continual moisture export from these regions by the horizontal divergence forced by the boundary-layer drag. This moisture, in turn, converges at the base of the WCB forced by surface drag and large-scale ageostrophic flow, thereby providing a substantial amount of moisture continuously to the WCB. Thus, the collocation of the LHF from the ocean and particle distributions is likely to indicate an active involvement of the moisture convergence associated with extratropical cyclones.

4.4 Typical synoptic conditions for individual moist particle pathways

The question remains as to what kind of synoptic conditions possibly give rise to different moist particle pathways. To answer this question, we have analyzed the particles trajectories of different moisture sources with the corresponding upper-tropospheric synoptic eddies. Great case-to-case spatiotemporal diversity is found in the associated synoptic fields, hampering their meaningful composite analyses (not shown). Instead, Figure 12 illustrates a more or less representative case that exhibits

https://doi.org/10.5194/wcd-2020-39
Preprint. Discussion started: 19 August 2020

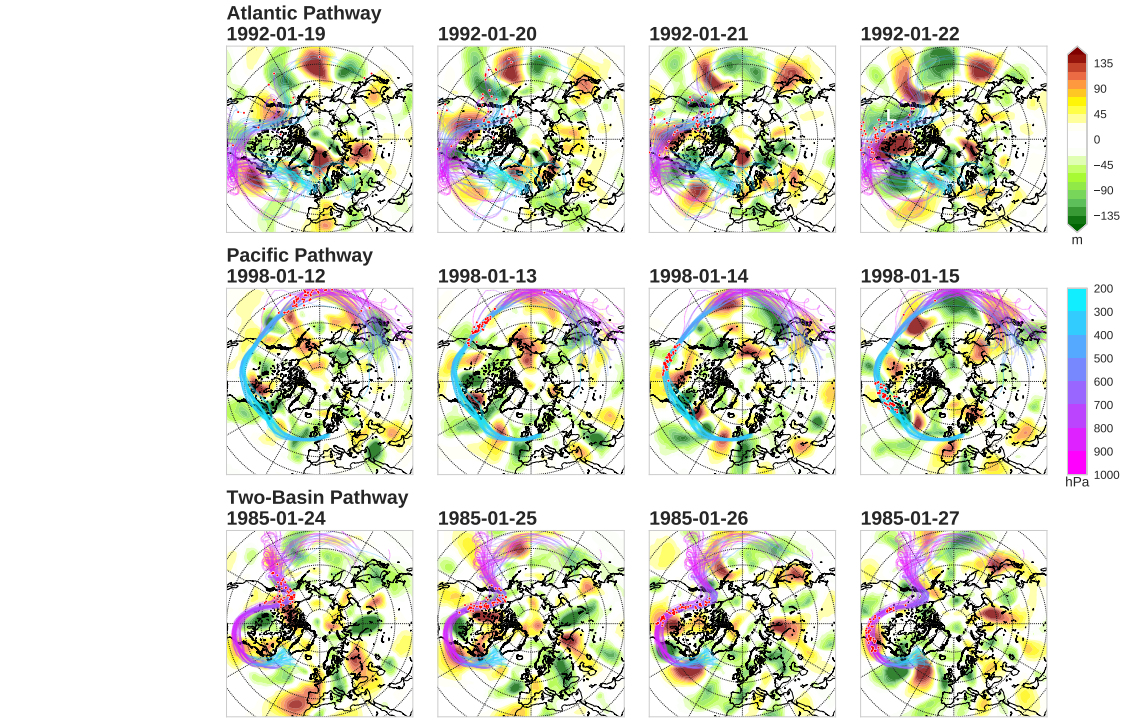

Figure 12. Case studies of particle locations (coloured lines) and associated synoptic-scale eddies (shaded as in the top right colour bar) for a case of the Atlantic pathway (top panels), the Pacific pathway (middle panel), and the two-basin pathway (bottom panel). The pressure levels [hPa] of up to 50 particles along their trajectories are plotted with coloured lines as indicated in the middle right colour bar. Their exact locations at the denoted times are indicated by red circles. The synoptic-scale eddies are defined as a 8-day high-pass filtered geopotential height fluctuations at 350 hPa.

the common features found for each pathway. Many cases are found to exhibit roughly similar properties to these representative cases.

One common feature for the vast majority of the Atlantic pathways is that the moist particles experience an organized descent over the North American continent oriented in the northwest-southeast direction in the vicinity of a synoptic-scale low-pressure system, before they gain moisture from the North Atlantic. These features well correspond to those associated with the dry intrusion, a deep descent of dry air from the upper atmosphere into the lower troposphere often associated with extratropical cyclones (Browning, 1997), as clearly presented in Figure 12 for January 22 1992 (top right-most panel). A climatological study conducted by Raveh-Rubin (2017) illustrates that the North American continent is one of the most prominent locations for dry intrusion air to start descending, before interacting with the warmer North Atlantic underneath approximately 48 hours later. Intrusion of a dry, cold atmospheric particle is likely to induce strong SHF and LHF from the North Atlantic, especially the warm Gulf Stream, as effective moistening of the particle before lifted up into an upper-level blocking anticyclone.

https://doi.org/10.5194/wcd-2020-39
Preprint. Discussion started: 19 August 2020

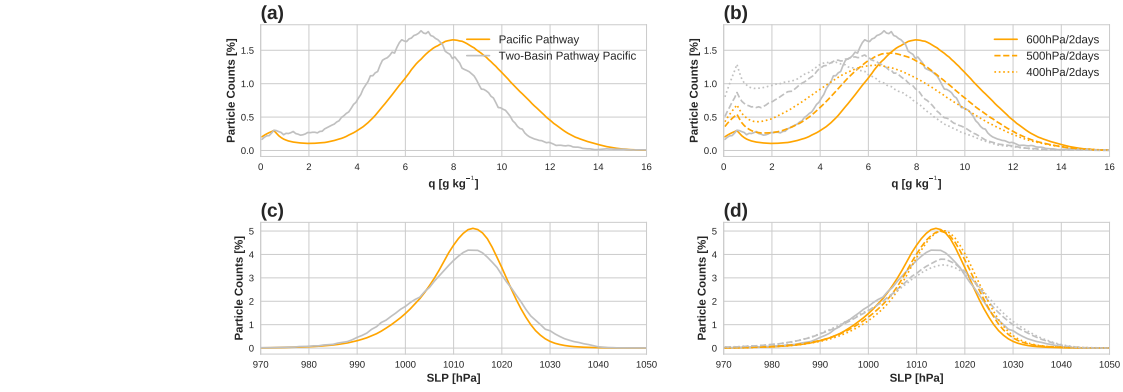

Figure 13. a) Specific humidity at the time of ascent for the Pacific pathway (orange) and two-basin pathway (grey). For the two-basin pathway, only the time of their ascent over the Pacific is considered for each particle. (b) Same as the panel (a) but for the different ascent criteria. (c) Same as (a) but for the sea level pressure found at the time of the ascent at the particle's horizontal location. (d) Same as the panel (c) but for the different ascent criteria.

Both the behaviour of trajectories and the associated synoptic conditions are fairly dissimilar for the Pacific pathways. Subsequent to large-scale ascent to the upper troposphere over the Pacific basin, the particles do not undergo deep descent over the North American continent unlike the Atlantic pathways. Instead, the particles appear to follow the upper-level westerly waveguide in the vicinity of blocking as can be seen on the panels on the second row of Figure 12. Although further investigation is required, this aspect appears to be consistent with the finding by Yamazaki and Itoh (2013b), who suggested that upper-level westerlies upstream of a blocking high can act as a waveguide to effectively carry synoptic anticyclones towards the blocking high.

All cases of the two-basin pathways are fairly analogous to the Atlantic pathways but extended farther upstream into the Pacific 10 days prior to the arrival at the blocking events. Compared to the Pacific pathways, the particles do not ascend as high off the west coast of North America, and as a result, they do not experience strong descent over the North American continent compared to the particles for the Atlantic pathways either. We found that this lack of strong ascent over the Pacific is likely attributable to the difference in moisture content of the particles. At the time of the ascent, the moisture content of the Pacific pathways is significantly higher than that of the two-basin pathways at the 95% confidence level, with the mean difference amounting to 1.4 g kg^{-1} (Figure 13a). This relationship between the ascent level and moisture content becomes more evident when a different ascent criterion is applied (Figure 13b). The figure reveals a clear link between the moisture content and the ascent level of a particle, in such a way that the higher the particle's moisture content at the base of the ascent, the higher the particle tends to ascend subsequently. In contrast, no such clear relationship is discernible with the sea-level pressure (SLP) found at the base of the particle ascent, despite that stronger low-pressure systems are likely associated with stronger ascent (Figures 13c, d). Although more careful analyses, including an investigation of the lowest SLP found in the vicinity of the ascent as included in the WCB detection (Madonna et al., 2014), are indispensable to draw a more solid conclusion, these

https://doi.org/10.5194/wcd-2020-39
Preprint. Discussion started: 19 August 2020

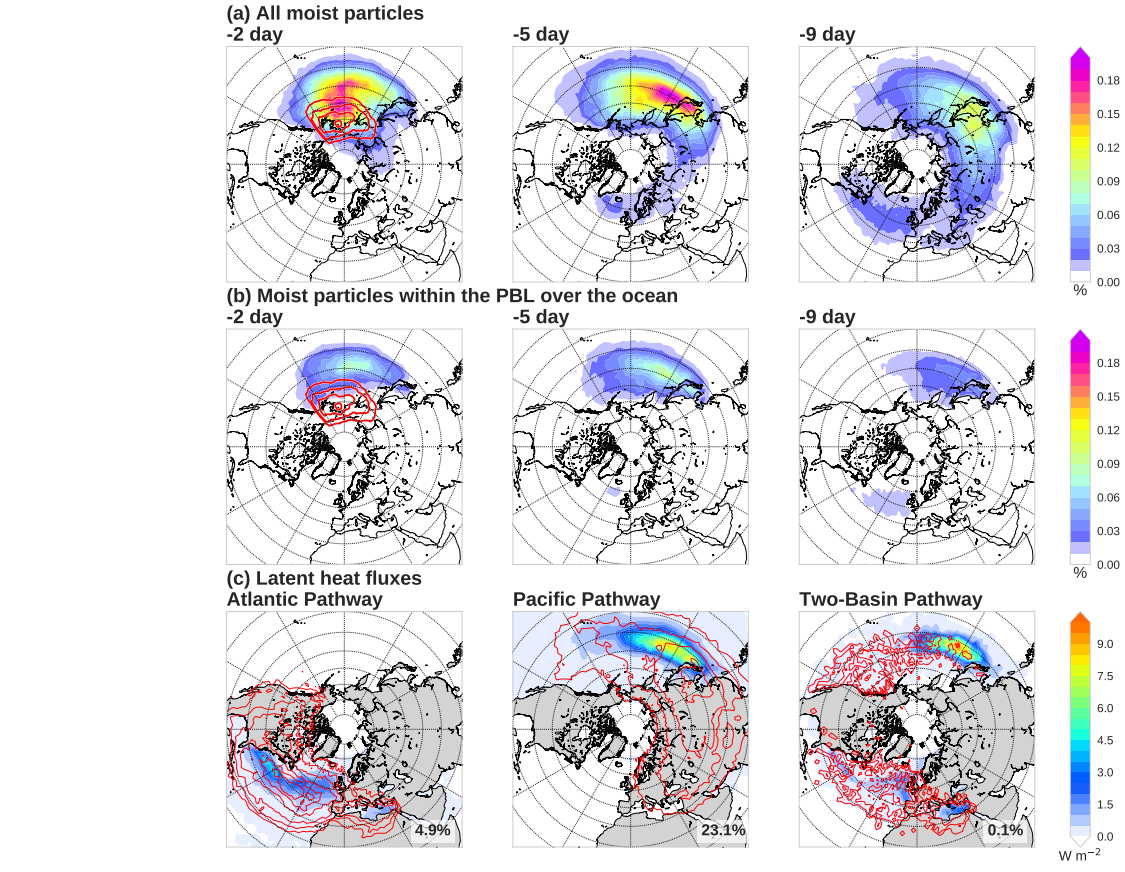

Figure 14. (1) Same as the top panels of Figure 2, but for the Pacific blocks. (b) Same as Figure 3(a), but for the Pacific blocks. (c) Same as Figure 7(a), but for the Pacific blocks. Locations of particles 10 days prior to the arrival at the blocks are overlaid on top for 0.01, 0.025, 0.05, 0,1, 0.15, and 0.2%. For the two-basin pathways only 0.01, 0.1, and 0.2% are indicated.

results point to the key role of the particles' moisture content, rather than the SLP, at the base of the ascent in determining their ascending altitude.

5 Comparison with the Pacific blocking

375 Finally, we briefly investigate the role of diabatic processes in Pacific blocking. Applying the same blocking index introduced in Section 2.2 for the DJF season over the domain [130°E - 140°W, 50°N - 75°N] (region encircled in Figure 1), approximately 4 million particles are released from the Pacific blocking grid cells at the altitudes between 7,000 and 8,000 m asl.

The fraction of the moist particles for the Pacific blocking is 28.6%. These moist particles are predominantly located over the Pacific basin, in particular just south of the blocking regions 2 days before the blocking occurrence and over the Kuroshio
380 Extension region 5 days prior to their arrival at the block (Figure 14a). The preferred locations of these moist particles when

https://doi.org/10.5194/wcd-2020-39
Preprint. Discussion started: 19 August 2020

located within the marine PBL are found in the vicinity of the Kuroshio Extension (Figure 14b). In stark contrast to the moist particles en route to the Euro-Atlantic blocking, which are under the effect of both of the western boundary currents (Figure 3), the Pacific counterparts do not show any noticeable sign of influence from the Gulf Stream and its extension (Figure 14b). Indeed, partitioning of the moist particles into different moisture sources reveals that the overwhelming majority (over 80%) of the moist particles source their moisture from the Pacific basin (Figure 14c), in contrast to 62.9% of moist particles from the Atlantic basin for the Euro-Atlantic blocking. In spite of the proximity, the Indian Ocean is still not a significant moisture source, amounting to only 0.1% of the moist particles. Thus, our results suggest that the Pacific blocking tends to source its moisture more locally.

This difference between the two blocking systems likely arises largely from the much greater zonal extent of the Eurasian continent than that of the North American continent, thereby making the North Atlantic basin less accessible. Furthermore, a comparison of the particle locations 9 days prior to the arrival at the blocking systems between the Pacific (Figure 14b) and the Euro-Atlantic (Figure 3) reveals that the Pacific particles are situated more poleward by about 10 degrees in latitude when located within the PBL over the Atlantic, thereby circumventing the warm Gulf Stream, a region of the recurrent development of extratropical cyclones necessary for large-scale uplift. Coupled with the narrowness of the North Atlantic basin compared to the Pacific basin, the Pacific particles seem to be less susceptible to the Atlantic Ocean. This constraint on the Atlantic pathways is somewhat mitigated when the particles are tracked for 20 days, where the fraction of the total moist particles increases to 47.1%, of which 13.3% is regarded as the Atlantic pathways, 27.4% as the Pacific pathways, and 0.05% as the two-basin pathways. Note that the vast majority of the remaining fraction is from the Arctic Ocean north of 65°N.

6 Discussion and Conclusion

Motivated by the previous studies which pointed towards the significance of latent heating for the atmospheric blocking events, we have investigated the oceanic moisture sources for the wintertime Euro-Atlantic blocking events. To this end, we have utilized an atmospheric Lagrangian dispersion model, which allows us to investigate the processes taking place within the turbulent planetary boundary layer (PBL). We found that approximately 36 - 55% of the total particles released from the wintertime Euro-Atlantic blocking highs undergo diabatic processes, gaining heat and moisture from the underlying ocean. Consistent with the previous studies, these moist particles transport significantly lower PV compared to dry particles from the PBL to the upper-tropospheric blocking highs via large-scale ascent. In stark contrast, dry particles travel pseudo-isobarically in the upper troposphere, while being cooled radiatively (Figure 5). PV values remains significantly different between the dry and the moist particles throughout their evolution even when they reach the blocking highs (Figure 5). As a consequence, there is a tendency for the moist particles to be preferentially concentrated in the blocking cores, indicating an important role of moist processes in the blocking systems (Figure 6).

Depending upon their moisture sources, the moist particles can be broadly divided into two categories: those via the Atlantic and via the Pacific. The former, locally-sourced particles, correspond to those that have been extensively studied in the previous studies (Pfahl et al., 2015; Steinfeld and Pfahl, 2019), which undergo a swift ascent a few days prior to their arrival

https://doi.org/10.5194/wcd-2020-39
Preprint. Discussion started: 19 August 2020

at the blocking systems. We have found that these particles tend to experience a large-scale descent over the North American continent, before efficiently gaining moisture from the North Atlantic (Figure 12 top row). Those particles that source their moisture remotely from the Pacific and then undergo ascent also transport low PV into the Euro-Atlantic blocking but almost in the same manner as the dry particles that travel along a westerly waveguide in the upper troposphere. PV of these moist particles remains significantly lower than the dry counterparts throughout, even all the way to their arrival at the blocking (Figure 8). In this sense, these moist particles can be regarded as a part of the class considered by Yamazaki and Itoh (2013a), such that anticyclonic low-PV particles are preferentially absorbed into the blocking system, acting to prolong the blocking lifetime. In their study, Yamazaki and Itoh (2013a) identified the mechanism by analyzing isentropic trajectories, and thus the involvement of moist processes remained uncertain. The current study, however, suggests that the same mechanism can be at play regardless of the source of low PV, thereby bridging the gap between the dry and the moist dynamical frameworks.

Our results further highlight that the paths that these moist particles preferentially follow while gaining moisture are concentrated over the western boundary currents as well as over the eastern Pacific to the north-east of the Hawaiian Islands (Figure 3 and Figure 7). These regions also coincide with the most frequent starting points of large-scale ascent within warm conveyor belts associated with extratropical cyclones (Figure 11). This collocation is likely linked with continuous evaporation from the warm sea surface and the subsequent transport toward the base of the warm conveyor belt associated with extratropical cyclones (Boutle et al., 2010). The western boundary currents are known for supplying a substantial amount of heat and moisture to the overlying atmosphere and thereby acting to anchor storm tracks by maintaining mean baroclinicity (Nakamura et al., 2004). Thus, given the primary role of the extratropical cyclones, it is not surprising that the enhanced latent heat fluxes and the starting positions of warm conveyor belts are collocated over the western boundary currents. Meanwhile, the region to the north-east of the Hawaiian Islands is not a region that is climatologically known for large upward latent heat fluxes nor a maximum in extratropical cyclone activity; rather, it corresponds to a region with an amplified vertically-integrated moisture flux divergence driven primarily by advection associated with intraseasonal variability of the Aleutian low (Newman et al., 2012; Kwon and Joyce, 2013). Whether this anomalous moisture advection associated with the intraseasonal variability of the Aleutian low is linked with moisture convergence at the base of the WCB as discussed by Boutle et al. (2010) requires further investigation in future analyses.

A brief comparison between the Atlantic and Pacific blocks revealed that the wintertime Pacific blocking is also under the influence of direct diabatic effect, albeit to a lesser extent compared to the Euro-Atlantic blocking. We have also found that the moist particles tend to source their moisture more locally compared to the Euro-Atlantic counterpart. This difference likely arises from the greater zonal extent of the Eurasian continent than that of the North American continent, impeding the influence from the Atlantic Ocean. We speculate that these differences associated with the moist processes may partly account for the difference seen between the Atlantic and Pacific blocking in their predictability and reproducibility in climate models (Matsueda et al., 2009; Matsueda, 2009).

Outstanding questions include whether the temporal variability of the western boundary currents on seasonal and longer time scales can affect blocking activity through modulations of moist processes. In this study we have focused on the climatological aspect of direct diabatic processes associated with blocking maintenance and shown that western boundary currents

https://doi.org/10.5194/wcd-2020-39
Preprint. Discussion started: 19 August 2020

provide a substantial amount of heat and moisture to the atmospheric particles en route to the Northern Hemisphere blocking systems. Observational evidence indicates that both the Kuroshio (Qiu and Chen, 2005; Kwon et al., 2010) and the Gulf Stream (McCarthy et al., 2018; Joyce et al., 2019) exhibit interannual and decadal variabilities, which have been shown to influence the overlying atmosphere, including blocking activity (O'Reilly and Czaja, 2015; Joyce et al., 2019). Whether these oceanic variabilities can modulate the direct diabatic processes associated with the blocking events described in the current study, however, is yet to be known. Hence in a subsequent study we will investigate the effect of the oceanic temporal variability. Given a recent study that showed the projected strengthening of the Kuroshio and weakening of the Gulf Stream under the future climate scenarios (Chen et al., 2019), understanding the sensitivity of the diabatic effect to the variabilities of these western boundary currents has important implications.

Appendix A: A hybrid blocking index

As is extensively discussed in Barriopedro et al. (2010) and Woollings et al. (2018), there is no one definite measure to define blocking and thus numerous definitions have been used in the literature. Each index aims to highlight different aspects of blocking systems, entailing its pros and cons. The two mainstream blocking indices include ones that detect the meridional gradient of geopotential height, focusing on the fact that blocks obstruct the prevailing westerlies (e.g., Tibaldi and Molteni, 1990; Scherrer et al., 2006) and others based on anomalies of variables such as geopotential height or potential vorticity from its climatological mean, highlighting that blocking highs are associated with strong anticyclonic anomalies (e.g., Dole and Gordon, 1983; Schwierz et al., 2004). Previous studies have reported that the former tends to erroneously detect the subtropical highs as blocks (Scherrer et al., 2006), while also having a deficiency in detecting omega or immature blocks (Doblas-Reyes et al., 2002; Pelly and Hoskins, 2003). The latter, in comparison, might suffer from cases when the geopotential height anomalies do not necessarily accompany a reversal of the westerlies (Woollings et al., 2018), while also having disadvantages in requiring arbitrary blocking anomaly thresholds and a robust climatology (Dunn-Sigouin et al., 2013).

In the current study, we identify blocks by using a hybrid index introduced by Dunn-Sigouin et al. (2013), which combines the basic ideas of both of these two types of blocking indices. Namely, blocks are detected by identifying a local maximum of 500-hPa geopotential height anomaly as was done in Dole and Gordon (1983), and then by ensuring that there exists a meridional height reversal around the identified maximum as in Tibaldi and Molteni (1990). More specifically, the following steps are followed:

1. 500-hPa geopotential height anomaly (Z') is computed by removing the climatological seasonal cycle and long-term variability as in Sausen et al. (1994) and then by imposing a weight proportional to the inverse of the sine of latitude. As such, Z' represents a quasi-geostrophic stream function anomaly.

2. Closed positive contours of Z' larger than a minimum amplitude threshold (A) with spatial scale (S) are then identified and tracked in time, ensuring that they meet the overlap criterion in blocking areas (O) for two consecutive days.

https://doi.org/10.5194/wcd-2020-39
Preprint. Discussion started: 19 August 2020

Weather and Climate Dynamics Discussions
Open Access
EGU

3. The existence of the reversal of the meridional gradient of the absolute 500-hPa geopotential height, defined as the maximum difference between the two grid points separated by a meridional range ($\Delta\phi$), is examined on the equatorial side of the anomaly maximum. The reversal criterion is met if the height gradient is negative at any longitude within a longitudinal range ($\Delta\lambda$).

4. The anomaly is identified as a blocking event if the above three criteria are met during a given period (D).

We have set the arbitrary thresholds to be identical to those used by Dunn-Sigouin et al. (2013): the amplitude threshold A of 1.5 standard deviations of Z' over 30 - 90°N computed for a period of 3-months centred at a given calendar month; the spatial scale S of 2.5 $\times$ 10^6 km^2; the overlap criterion O of 50%; the meridional $\Delta\phi$ and zonal $\Delta\lambda$ scales of 15° in latitude and 10° in longitude, respectively; and the duration period D of 5 days. These choices of criteria are rather restrictive and, as a result, tend to highlight the mature/maintenance stage of blocking. The usage of these criteria can suppress the erroneous detection of quasi-stationary ridges and immature systems as blocks, while well capturing omega-shaped blocking, thereby overcoming the shortcomings of the previously used indices (Dunn-Sigouin et al., 2013).

Appendix B: Atmospheric dispersion model FLEXPART

FLEXPART is a comprehensive offline atmospheric Lagrangian dispersion model, widely used for diverse atmospheric transport applications. FLEXPART computes the particle trajectories under the assumption of zero acceleration as

$$\mathbf{X}(t+\Delta t) = \mathbf{X}(t) + \mathbf{v}(\mathbf{X},t)\Delta t, \tag{B1}$$

where t denotes time, Δt the time increment, and $\mathbf{X}$ the particle's position vector. $\mathbf{v} = \overline{\mathbf{v}} + \mathbf{v}_t + \mathbf{v}_m$, is the three-dimensional wind vector consisting of grid-scale winds ($\overline{\mathbf{v}}$), turbulent wind fluctuations ($\mathbf{v}_t$), and mesoscale wind fluctuations ($\mathbf{v}_m$). Turbulent wind fluctuations are evaluated by solving Langevin equations (Thomson, 1987) in assuming Gaussian turbulence. Mesoscale wind fluctuations, whose spectral interval falls between the resolved winds and the turbulent wind fluctuations, are approximated by solving an independent Langevin equation for the mesoscale wind velocity fluctuations in a similar manner to Maryon et al. (1998).

In addition, in FLEXPART, one can optionally evaluate the effect of moist convective transport that takes place within convective clouds by turning on the moist convection scheme by Emanuel and Živković-Rothman (1999), at the expense of the substantial increase in the computational time (Stohl et al., 2005). This transport is grid-scale in the vertical but subgrid-scale in the horizontal. A recent study by Oertel et al. (2020) has highlighted the importance of convection embedded in WCBs by using a high-resolution model with a 0.02° horizontal resolution. Switching on the moist convection scheme in FLEXPART, however, does not qualitatively or quantitatively alter our results, suggesting that the importance of the subgrid-scale horizontal convection is only secondary to the resolved grid-scale convection in the current study with a much coarser resolution (not shown). For this reason, we turn off the moist convection scheme in our analyses.

https://doi.org/10.5194/wcd-2020-39
Preprint. Discussion started: 19 August 2020

Weather and Climate Dynamics Discussions
Open Access
EGU

Author contributions. A.Yamamoto designed the study in discussion with Y-O.K. and performed the analysis. All authors contributed to interpreting the results and writing the manuscript.

Competing interests. The authors declare that they have no conflict of interest.

Acknowledgements. We would like to thank E. Dunn-Sigouin for kindly providing us with the original blocking detection code. The earlier version of the manuscript was significantly improved thanks to the insightful comments from C. Grams and A. Czaja. The support for this work was provided by the Japan Society for the Promotion of Science (JSPS) KAKENHI Grants JP19H05704, JP19H05702 and JP19H05703 (on Innovative Areas 6102), by the Japan Science and Technology Agency through Belmont Forum CRA “InterDec", by the Japanese Ministry of Environment through Environment Research and Technology Development Fund 2-1904, and by and the Japanese Ministry of Education, Culture, Sports, Science and Technology (MEXT) through the Arctic Challenge for Sustainability (ArCS and ARCS II) programs. P.M. was partly supported by Grant-in-Aid for JSPS Research Fellow. Y-O.K. gratefully acknowledges support from US DOE CESD Regional and Gloabal Model Analysis Program (DE-SC0019492).

https://doi.org/10.5194/wcd-2020-39
Preprint. Discussion started: 19 August 2020

Weather and Climate Dynamics Discussions
Open Access
EGU

References

Barriopedro, D., García-Herrera, R., and Trigo, R. M.: Application of blocking diagnosis methods to General Circulation Models. Part I: a novel detection scheme, Climate Dynamics, 35, 1373–1391, https://doi.org/10.1007/s00382-010-0767-5, 2010.

Booth, J. F., Dunn-Sigouin, E., and Pfahl, S.: The Relationship Between Extratropical Cyclone Steering and Blocking Along the North American East Coast, Geophysical Research Letters, 44, 11,976–11,984, https://doi.org/10.1002/2017GL075941, 2017.

Boutle, I. A., Beare, R. J., Belcher, S. E., Brown, A. R., and Plant, R. S.: The moist boundary layer under a mid-latitude weather system, Boundary-Layer Meteorology, 134, 367–386, https://doi.org/10.1007/s10546-009-9452-9, 2010.

Browning, K. A.: The dry intrusion perspective of extra-tropical cyclone development, Meteorological Applications, 4, 317–324, https://doi.org/10.1017/S1350482797000613, 1997.

Chen, C., Wang, G., Xie, S.-P., and Liu, W.: Why Does Global Warming Weaken the Gulf Stream but Intensify the Kuroshio?, Journal of Climate, 32, 7437–7451, https://doi.org/10.1175/jcli-d-18-0895.1, 2019.

Croci-Maspoli, M. and Davies, H. C.: Key Dynamical Features of the 2005/06 European Winter, Monthly Weather Review, 137, 664–678, https://doi.org/10.1175/2008mwr2533.1, 2008.

Davini, P. and D'Andrea, F.: Northern Hemisphere atmospheric blocking representation in global climate models: Twenty years of improvements?, Journal of Climate, 29, 8823–8840, https://doi.org/10.1175/JCLI-D-16-0242.1, 2016.

Doblas-Reyes, F. J., Casado, M. J., and Pastor, M. A.: Sensitivity of the Northern Hemisphere blocking frequency to the detection index, Journal of Geophysical Research Atmospheres, 107, 4009, https://doi.org/10.1029/2000jd000290, 2002.

Dole, R. M. and Gordon, N. D.: Persistent anomalies of the extratropical Northern Hemisphere wintertime circulation: structure., Monthly Weather Review, 111, 1567–1586, https://doi.org/10.1175/1520-0493(1986)114<0178:PAOTEN>2.0.CO;2, 1983.

Dunn-Sigouin, E., Son, S.-W., and Lin, H.: Evaluation of Northern Hemisphere Blocking Climatology in the Global Environment Multi-scale Model, Monthly Weather Review, 141, 707–727, https://doi.org/10.1175/MWR-D-12-00134.1, http://journals.ametsoc.org/doi/abs/10.1175/MWR-D-12-00134.1, 2013.

Emanuel, K. A. and Živković-Rothman, M.: Development and Evaluation of a Convection Scheme for Use in Climate Models, Journal of the Atmospheric Sciences, 56, 1766–1782, https://doi.org/10.1175/1520-0469(1999)056<1766:DAEOAC>2.0.CO;2, http://journals.ametsoc.org/doi/abs/10.1175/1520-0469{%}281999{%}29056{%}3C1766{%}3ADAEOAC{%}3E2.0.CO{%}3B2, 1999.

Grams, C. M., Wernli, H., Böttcher, M., Čampa, J., Corsmeier, U., Jones, S. C., Keller, J. H., Lenz, C. J., and Wiegand, L.: The key role of diabatic processes in modifying the upper-tropospheric wave guide: A North Atlantic case-study, Quarterly Journal of the Royal Meteorological Society, 137, 2174–2193, https://doi.org/10.1002/qj.891, 2011.

Häkkinen, S., Rhines, P. B., and Worthen, D. L.: Atmospheric blocking and Atlantic multidecadal ocean variability., Science (New York, N.Y.), 334, 655–9, https://doi.org/10.1126/science.1205683, 2011.

Joyce, T. M., Kwon, Y.-O., Seo, H., and Ummenhofer, C. C.: Meridional Gulf Stream Shifts Can In fluence Wintertime Variability in the North Atlantic Storm Track and Greenland Blocking, Geophysical Research Letters, 46, 1702–1708, https://doi.org/10.1029/2018GL081087, https://doi.org/10.1029/2018GL081087, 2019.

Kwon, Y. O. and Joyce, T. M.: Northern hemisphere winter atmospheric transient eddy heat fluxes and the gulf stream and Kuroshio-Oyashio extension variability, Journal of Climate, 26, 9839–9859, https://doi.org/10.1175/JCLI-D-12-00647.1, http://journals.ametsoc.org/doi/abs/10.1175/JCLI-D-12-00647.1, 2013.

https://doi.org/10.5194/wcd-2020-39
Preprint. Discussion started: 19 August 2020

Kwon, Y.-O., Alexander, M. A., Bond, N. A., Frankignoul, C., Nakamura, H., Qiu, B., and Thompson, L.: Role of the Gulf Stream and Kuroshio-Oyashio systems in large-scale atmosphere-ocean interaction: A review, Journal of Climate, 23, 3249–3281, https://doi.org/10.1175/2010JCLI3343.1, 2010.

Kwon, Y.-O., Seo, H., Ummenhofer, C. C., and Joyce, T. M.: Impact of Multidecadal Variability in Atlantic SST on Winter Atmospheric Blocking, Journal of Climate, 33, 867–892, https://doi.org/10.1175/JCLI-D-19-0324.1, http://journals.ametsoc.org/doi/10.1175/JCLI-D-19-0324.1, 2020.

Madonna, E., Wernli, H., Joos, H., and Martius, O.: Warm conveyor belts in the ERA-Interim Dataset (1979-2010). Part I: Climatology and potential vorticity evolution, Journal of Climate, 27, 3–26, https://doi.org/10.1175/JCLI-D-12-00720.1, 2014.

Maryon, R. H., Ltd, E. S., and Maryon, R. H.: Determining cross-wind variance for low frequency wind meander, Atmospheric Environment, 32, 115–121, 1998.

Masato, G., Hoskins, B. J., and Woollings, T. J.: Wave-breaking characteristics of midlatitude blocking, Quarterly Journal of the Royal Meteorological Society, 138, 1285–1296, https://doi.org/10.1002/qj.990, 2012.

Matsueda, M.: Blocking predictability in operational medium-range ensemble forecasts, Scientific Online Letters on the Atmosphere, 5, 113–116, https://doi.org/10.2151/sola.2009-029, 2009.

Matsueda, M., Mizuta, R., and Kusunoki, S.: Future change in wintertime atmospheric blocking simulated using a 20-km-mesh atmospheric global circulation model, Journal of Geophysical Research Atmospheres, 114, 1–10, https://doi.org/10.1029/2009JD011919, 2009.

McCarthy, G. D., Joyce, T. M., and Josey, S. A.: Gulf Stream variability in the context of quasi-decadal and multi-decadal Atlantic climate variability, Geophysical Research Letters, 45, https://doi.org/10.1029/2018GL079336, http://doi.wiley.com/10.1029/2018GL079336, 2018.

Methven, J.: Potential vorticity in warm conveyor belt outflow, Quarterly Journal of the Royal Meteorological Society, 141, 1065–1071, https://doi.org/10.1002/qj.2393, 2015.

Nakamura, H.: Rotational evolution of potential vorticity associated with a strong blocking flow configuration over Europe, Geophysical Research Letters, 21, 2003–2006, https://doi.org/10.1029/94GL01614, 1994.

Nakamura, H. and Fukamachi, T.: Evolution and dynamics of summertime blocking over the Far East and the associated surface Okhotsk high, Quarterly Journal of the Royal Meteorological Society, 130, 1213–1233, https://doi.org/10.1256/qj.03.101, 2004.

Nakamura, H., Nakamura, M., and Anderson, J. L.: The Role of High- and Low-Frequency Dynamics in Blocking Formation, Monthly Weather Review, 125, 2074–2093, https://doi.org/10.1175/1520-0493(1997)125<2074:trohal>2.0.co;2, 1997.

Nakamura, H., Sampe, T., Tanimoto, Y., and Shimpo, A.: Observed Associations Among Storm Tracks, Jet Streams and Midlatitude Oceanic Fronts, in: Earth's Climate: The Ocean-Atmosphere Interaction, edited by Wang, C., Xie, S.-P., and Carton, J. A., pp. 329–346, American Geophysical Union, Washington, D.C., U.S.A., https://doi.org/10.1029/147GM18, 2004.

Newman, M., Kiladis, G. N., Weickmann, K. M., Ralph, M. F., and Sardeshmukh, P. D.: Relative contributions of synoptic and low-frequency eddies to time-mean atmospheric moisture transport, including the role of atmospheric rivers, Journal of Climate, 25, 7341–7361, https://doi.org/10.1175/JCLI-D-11-00665.1, 2012.

Novak, L., Ambaum, M. H., and Tailleux, R.: The life cycle of the North Atlantic storm track, Journal of the Atmospheric Sciences, 72, 821–833, https://doi.org/10.1175/JAS-D-14-0082.1, 2015.

Oertel, A., Boettcher, M., Joos, H., Sprenger, M., and Wernli, H.: Potential vorticity structure of embedded convection in a warm conveyor belt and its relevance for the large-scale dynamics, Weather and Climate Dynamics, 1, 127–153, https://doi.org/10.5194/wcd-1-127-2020, 2020.

https://doi.org/10.5194/wcd-2020-39
Preprint. Discussion started: 19 August 2020

O'Reilly, C. H. and Czaja, A.: The response of the pacific storm track and atmospheric circulation to kuroshio extension variability, Quarterly Journal of the Royal Meteorological Society, 141, 52–66, https://doi.org/10.1002/qj.2334, 2015.

O'Reilly, C. H., Minobe, S., and Kuwano-Yoshida, A.: The influence of the Gulf Stream on wintertime European blocking, Climate Dynamics, 47, 1545–1567, https://doi.org/10.1007/s00382-015-2919-0, 2016.

Pelly, J. L. and Hoskins, B. J.: A new perspective on blocking, Journal of the Atmospheric Sciences, 60, 743–755, https://doi.org/10.1175/1520-0469(2003)060<0743:ANPOB>2.0.CO;2, 2003.

Pfahl, S., Schwierz, C., Grams, C. M., Wernli, H., Croci-Maspoli, M., Grams, C. M., and Wernli, H.: Importance of latent heat release in ascending air streams for atmospheric blocking, Nature Geoscience, 8, 610–615, https://doi.org/10.1038/NGEO2487, 2015.

Qiu, B. and Chen, S.: Eddy-Induced Heat Transport in the Subtropical North Pacific from Argo, TMI, and Altimetry Measurements, Journal of Physical Oceanography, 35, 458–473, https://doi.org/10.1175/JPO2696.1, http://journals.ametsoc.org/doi/abs/10.1175/JPO2696.1, 2005.

Raveh-Rubin, S.: Dry intrusions: Lagrangian climatology and dynamical impact on the planetary boundary layer, Journal of Climate, 30, 6661–6682, https://doi.org/10.1175/JCLI-D-16-0782.1, 2017.

Rex, D. F.: Blocking Action in the Middle Troposphere and its Effect upon Regional Climate, Tellus, 2, 275–301, https://doi.org/10.3402/tellusa.v2i4.8603, 1950.

Saha, S., Moorthi, S., Pan, H.-L., Wu, X., Wang, J., Nadiga, S., Tripp, P., Kistler, R., Woollen, J., Behringer, D., Liu, H., Stokes, D., Grumbine, R., Gayno, G., Wang, J., Hou, Y.-T., Chuang, H.-y., Juang, H.-M. H., Sela, J., Iredell, M., Treadon, R., Kleist, D., Van Delst, P., Keyser, D., Derber, J., Ek, M., Meng, J., Wei, H., Yang, R., Lord, S., van den Dool, H., Kumar, A., Wang, W., Long, C., Chelliah, M., Xue, Y., Huang, B., Schemm, J.-K., Ebisuzaki, W., Lin, R., Xie, P., Chen, M., Zhou, S., Higgins, W., Zou, C.-Z., Liu, Q., Chen, Y., Han, Y., Cucurull, L., Reynolds, R. W., Rutledge, G., and Goldberg, M.: The NCEP Climate Forecast System Reanalysis, Bulletin of the American Meteorological Society, 91, 1015–1057, https://doi.org/10.1175/2010BAMS3001.1, http://journals.ametsoc.org/doi/10.1175/2010BAMS3001.1, 2010.

Sausen, R., König, W., and Sielmann, F.: Analysis of blocking events from observations and ECHAM model simulations, Tellus, Series A: Dynamic Meteorology and Oceanography, 47, 421–438, https://doi.org/10.3402/tellusa.v47i4.11526, 1994.

Scaife, A. A., Copsey, D., Gordon, C., Harris, C., Hinton, T., Keeley, S., O'Neill, A., Roberts, M., and Williams, K.: Improved Atlantic winter blocking in a climate model, Geophysical Research Letters, 38, L23 703, https://doi.org/10.1029/2011GL049573, http://doi.wiley.com/10.1029/2011GL049573, 2011.

Scherrer, S. C., Croci-Maspoli, M., Schwierz, C., and Appenzeller, C.: Two-dimensional indices of atmospheric blocking and their statistical relationship with winter climate patterns in the Euro-Atlantic region, International Journal of Climatology, 26, 233–249, https://doi.org/10.1002/joc.1250, 2006.

Schwierz, C., Croci-Maspoli, M., and Davies, H. C.: Perspicacious indicators of atmospheric blocking, Geophysical Research Letters, 31, L06 125, https://doi.org/10.1029/2003gl019341, 2004.

Sheldon, L., Czaja, A., Vannière, B., Morcrette, C., Sohet, B., Casado, M., and Smith, D.: A 'warm path' for Gulf Stream-troposphere interactions, Tellus, Series A: Dynamic Meteorology and Oceanography, 69, 1–15, https://doi.org/10.1080/16000870.2017.1299397, http://dx.doi.org/10.1080/16000870.2017.1299397, 2017.

Shutts, G. J.: The propagation of eddies in diffluent jetstreams: Eddy vorticity forcing of 'blocking' flow fields, Quarterly Journal of the Royal Meteorological Society, 109, 737–761, https://doi.org/10.1002/qj.49710946204, 1983.

https://doi.org/10.5194/wcd-2020-39
Preprint. Discussion started: 19 August 2020

Steinfeld, D. and Pfahl, S.: The role of latent heating in atmospheric blocking dynamics: a global climatology, Climate Dynamics, 53, 6159–6180, https://doi.org/10.1007/s00382-019-04919-6, https://doi.org/10.1007/s00382-019-04919-6http://link.springer.com/10.1007/s00382-019-04919-6, 2019.

Stohl, A., Forster, C., Frank, A., Seibert, P., and Wotawa, G.: Technical note: The Lagrangian particle dispersion model FLEXPART version 6.2, Atmospheric Chemistry and Physics, 5, 2461–2474, https://doi.org/10.5194/acp-5-2461-2005, www.atmos-chem-phys.org/acp/5/2461/http://www.atmos-chem-phys.net/5/2461/2005/, 2005.

Thomson, D. J.: Criteria for the selection of stochastic models of particle trajectories in turbulent flows, Journal of Fluid Mechanics, 180, 529–556, https://doi.org/10.1017/S0022112087001940, http://www.journals.cambridge.org/abstract{_}S0022112087001940, 1987.

Tibaldi, S. and Molteni, F.: On the operational predictability of blocking, Tellus, 42A, 343–365, https://doi.org/10.1034/j.1600-0870.1990.t01-2-00003.x, 1990.

Wernli, H. and Davies, H. C.: A Lagrangian-based analysis of extratropical cyclones. I: The method and some applications, Quarterly Journal of the Royal Meteorological Society, 123, 467–489, https://doi.org/10.1256/smsqj.53810, 1997.

Woollings, T., Barriopedro, D., Methven, J., Son, S. W., Martius, O., Harvey, B., Sillmann, J., Lupo, A. R., and Seneviratne, S.: Blocking and its Response to Climate Change, Current Climate Change Reports, 4, 287–300, https://doi.org/10.1007/s40641-018-0108-z, 2018.

Yamamoto, A. and Palter, J. B.: The absence of an Atlantic imprint on the multidecadal variability of wintertime European temperature., Nature communications, 7, 10 930, https://doi.org/10.1038/ncomms10930, http://www.nature.com/ncomms/2016/160315/ncomms10930/full/ncomms10930.html, 2016.

Yamamoto, A., Palter, J. B., Lozier, M. S., Bourqui, M. S., and Leadbetter, S. J.: Ocean versus atmosphere control on western European wintertime temperature variability, Climate Dynamics, 45, 3593–3607, https://doi.org/10.1007/s00382-015-2558-5, http://link.springer.com/10.1007/s00382-015-2558-5, 2015.

Yamazaki, A. and Itoh, H.: Vortex–Vortex Interactions for the Maintenance of Blocking. Part I: The Selective Absorption Mechanism and a Case Study, Journal of the Atmospheric Sciences, 70, 725–742, https://doi.org/10.1175/JAS-D-11-0295.1, http://journals.ametsoc.org/doi/abs/10.1175/JAS-D-11-0295.1, 2013a.

Yamazaki, A. and Itoh, H.: Vortex-vortex interactions for the maintenance of blocking. part II: Numerical experiments, Journal of the Atmospheric Sciences, 70, 743–766, https://doi.org/10.1175/JAS-D-12-0132.1, 2013b.